Intersubband lifetimes and free carrier effects in optically pumped far infrared quantum wells laser structures

H. A. Tan, Z. –J. Xin and H. N. Rutt

Optoelectronics Research Centre, University of Southampton,

Southampton SO17 1BJ, United Kingdom

J. –P. R. Wells and I. V. Bradley

FOM-Institute for Plasma Physics "Rijnhuizen", P. O. Box 1207,

NL-3430 BE Nieuwegein, The Netherlands

Electron intersubband lifetimes of 1.8 ps and 2.5 ps were measured in GaAs/AlGaAs stepped quantum well samples by using a pump-probe three-beam technique at 4K to room temperature. At saturation pump intensities, an absorptive signal of sub-nanosecond lifetime was detected following a normal positive transmissive signal of picosecond lifetime. This absorptive signal is believed to be caused by the absorption from the free electrons pumped from the ground subband to the continuum conduction band in the barrier layers associated with incoherent two-photon process. The intersubband lifetimes and free carrier effects play an important role in optically pumped multiple-quantum-well far infrared lasers. A three-level electron transition model is built to simulate the process, which agrees very well with the experimental data.

1. INTRODUCTION

In a symmetric quantum well (QW), electrons can only make photon-induced transitions between subbands with an odd difference in their quantum number. This rule can be broken in an asymmetric QW, for example, a stepped QW. Asymmetric QWs have found uses in infrared photo-detectors [1] and proposed optically pumped intersubband far-infrared (FIR) lasers [2-4]. In the latter, the laser relies on the achievement of a population inversion between the second excited subband, to which the electrons in the ground subband are optically pumped, and the first excited

subband. The estimated threshold pump power is in the region of 100 kW/cm^2 [2]. In this case, the electrons in the excited subbands can be well away from the equilibrium (lattice) temperature and become hot electrons. This can significantly increase non-radiative transition rates, particularly by emission of longitudinal optical phonons, and consequently shorten the lifetime of the electron in the second excited subband. It is thus crucial to know the electron behaviour at high pump intensities. Time resolved measurements in intersubband lifetimes in QWs have been studied extensively for the past two decades [5-9]. In particular, Gauthier-Lafaye et al [9] have demonstrated a stimulated emission and gain at $\lambda \approx 12.5$ μm with intersubband energy greater than the longitudinal optical (LO) phonon energy. The energy difference between the first two excited subbands in our structures is less than the LO phonon energy, which will result in a greater free carrier absorption due to a λ^2 dependence. In this paper we report measurements of the kinetics of our intersubband FIR system using a picosecond pump-probe technique.

2. EXPERIMENTAL SETUP

The experiment was conducted using a free electron laser (FELIX) which produces high peak power, picosecond pulses widely tunable across the infrared spectral region. A pump-probe three-beam technique was applied to measure electron intersubband lifetime. The laser pulses were firstly split into two parts with a ratio 95%:5%. The stronger part was used as a pump; while the weaker part was further split into a probe and reference of equal intensity. The reference pulse was then delayed for 20 nanoseconds with respect to its original probe pulse and back reflected using a -1 telescope onto the probe beam path. The mercury-cadmium-telluride detector used to detect the transmission of the probe was biased using an RF signal

phase locked to the FEL output. The detector is thus positive biased for the probe signal and negative biased for the reference signal. Integration of the detector output then provides suppression of noise caused by power fluctuations of the FEL micro-pulses within the macropulse. The set-up was described in detail in Ref. 10. The micro-pulse output of the laser can be of sub-picoseconds and peak intensity of tens of MW/cm^2 [11]

Two $GaAs/Al_xGa_{1-x}As$ samples were used in this work containing 80 and 50 periods of stepped QWs respectively. The nominal parameters and corresponding potential structure for sample one are illustrated in figure 1. This sample was doped with silicon at a concentration of $2\times10^{17}/cm^3$ and a thickness of 5 nm in the middle of the barriers. We have utilised a one-dimensional model which calculated self-consistently the Schrödinger and Poisson equations [12]. The energy difference from the ground level to the second excited level, ΔE_{02} is 124 meV to allow the use of a tunable CO_2 laser pump. The energy difference between the first two excited subbands, ΔE_{12} is 23 meV. The TM polarized pump and probe beams had an angle of incidence of 30° and 60° respectively to the normal of the sample. The sample was mounted in a liquid helium gas flow cryostat whose temperature is variable from 4K to above room temperature.

3. RESULTS AND DISCUSSION

Figure 2 shows the differential transmission signal of the probe pulse as a function of the delay time relative to the pump pulse at a pump wavelength of 10.6 μm. This data was taken at a temperature of 4.2 K from the pump-probe experiment on sample one. Wavelength scans showed that the strongest differential transmission signal was found at pump wavelength of 10.6 μm as shown in the inset of figure 2. This pump wavelength is longer than the wavelength λ_{02} = 10.0 μm at which the optical transition from the ground to the second excited subband takes place, while

shorter than wavelength $\lambda_{01} = 12.3$ μm at which the optical transition from the ground to the first excited subband occurs. Thus the strongest differential transition at this pump wavelength can be attributed to the spectral overlap between the two transitions ΔE_{02} and ΔE_{01}.

A 5 dB attenuator was used at the laser output in the measurement in figure 2. The decay signal corresponds to a 1.8 ps lifetime as fitted by the bolder line. This value is several times longer than that obtained from rectangular QWs [7,8,13,14]. This can be attributed to the fact that the overlap of the wavefunctions in a stepped QW for the intersubband transition concerned is smaller compared to that in a rectangular QW.

Interestingly enough, with increasing pump power, a strong absorptive signal started to appear, which immediately followed the short positive decay (τ_1) but decreased much more slowly as shown in figure 3. A close study of the curves in figure 3 found that the decay consists of three components, τ_1 corresponds to a conventional pump-probe signal as shown in figure 2, τ_2 with a time scale of few hundred picoseconds and τ_3 lasting also hundreds of picoseconds but longer than τ_2. τ_3 has an astonishingly long lifetime of 550 ps for sample one, which is compared with normal electron intersubband lifetime of around a picosecond.

Figure 4 shows more data of the differential transmission signals, showing the dependence of the slow decay on the pump power, wavelengths and temperatures respectively. The data taken for this figure was obtained from sample two. This sample has a similar structure as the one given in figure 1 and used in figures 2 and 3, but with a much heavier doping ($2\times10^{18}/cm^3$) and lower barrier ($x = 0.35$). Spectral measurement at 6 K showed for this sample $\Delta E_{02} = 135$ meV and $\Delta E_{01} = 126$ meV. An intersubband lifetime of 2.5 ps was obtained for sample two.

For clarity, the curves in figure 4 have been shifted vertically from their zero level. We notice in the figure that the slow decay feature does not disappear until above 10 dB attenuation and 12.55 μm pump wavelength, although the peaks at the zero time delay are still visible for those measurements. The absolute power density incident on sample one was much higher than that for sample two as a result of more careful optical alignment and a wider spectrum of the FELIX pump pulse.

The strong intensity dependence and disappearance at longer wavelengths of the slow decay suggest that an incoherent two-photon process may be involved in the pump-probe experiment at intensities approaching pump saturation. At very high pump intensities, the first transition subband of the sample can be populated to saturation when the positive differentially transmissive peak appears. Following that, a considerable number of electrons in this excited subband can be further pumped out to the continuum or quasi-continuum conduction band. These free electrons are able to perform 3-D absorption, which is much stronger than the absorption taking place in 2-D environment since the selection rules have been relaxed. The stronger 3-D absorption can eventually outweigh the absorption decrease caused by the ground subband electron depopulation. A schematic illustration for the process is depicted in figure 5.

To test this explanation, we rearranged our experiment so that the incident angle of the probe beam was at 0° (normal to the sample) and the incident angle of the pump beam remained nonzero (we used 25°). The probe beam will now have no response to any variation of the electron population in a subband, but will strongly dependent on the population of 3-D free electrons in the continuum conduction band. As a result, only the negative signal was detected in this geometry, confirming the assignments. Also in this case, because of the electric vector of pump and probe

beams has a large component in the QW plane, any effect on the intersubband lifetime measurement due to intrasubband absorption [15] should be detectable. However, there was no perceivable positive signal in this case, which suggests that any intrasubband effect contribution were negligible to the intersubband lifetime measurement.

The lifetime of the electrons out of the wells can be prolonged by the distortion of the conduction band in the barrier layers due to modulation doping as shown in figure 5. The electrons pumped to the top of the QWs therefore can quickly diffuse and drift to the doping region under the forces induced by chemical and electrical potentials. This spatial separation of the excited photoelectrons from the QWs plus the rectifying potential can significantly delay their recombination time to the empty states in the QWs, which is normally in the region of a picosecond [1]. This is why τ_3 in figure 3 (sample one) is shorter than that in figure 4 (sample two) as the later had a much higher doping concentration. Furthermore, the energy gap between the ground subband and the bottom of the continuum conduction band (ΔE_{c0} in figure 5) for sample two is closer to the two-photon resonant energy than that in sample one. Consequently, even though the pumping power intensity for sample one was much stronger than that for sample two, sample two still needed a larger attenuation to totally suppress the negative signal. Intersubband two-photon transitions from the ground subband to the continuum state [16] and electromagnetically induced two photon resonant between subbands [17] have been demonstrated previously in symmetric QWs. In addition, the result in which the 3-D absorption feature was independent of temperature variations from 4K to 300K can be attributed to the background thermal radiation because of large view field of the sample.

Due to overlap of the absorption spectra of ΔE_{01} and ΔE_{02}, the pump transition of the electrons may no longer necessarily occur between the ground and second excited subbands. However the analysis here and the above is still applicable. We have considered the possibility that the second order nonlinear effect [18,19] could be involved in the experiment due to the asymmetric quantum well structure in addition to very high pump power intensity. In particular this nonlinear effect can be enhanced due to the fact that the energy difference of the ground subband to the bottom of the continuum conduction band in the barrier layers is 264 meV which is coincident with the resonant energy of the second harmonic generation. Short wave pass filters (CaF_2) added in front of the detector showed no evidence of appreciable second harmonic generation, although care must be taken with significant levels of FEL harmonic radiation in the pump beam. These can readily be confused with genuine second harmonic signals.

4. MODELLING

In order to investigate the feasibility of the two-photon mechanism, we established a three-level model to simulate the process, i.e. the ground subband, excited subband and continuum conduction band as seen in figure 1. In the model E_0 denotes the ground subband; E_i the excited subbands, which could be the higher excited subbands in our quantum well structure; the continuum band is represented as E_c, the third level in this model. This incoherent two-photon absorption model is valid for the pump-probe analysis, since the electron dephasing time in semiconductor quantum wells is generally shorter than the intersubband lifetime [13,14].

The 3-level system model comprises the rate equations and an equation for total population, shown here as Equations 1-3. In these equations, N_0, N_i and N_c represent the electron populations in the ground and excited levels as well as

continuum conduction band respectively. The total electron population is N, which is calculated from the Si doping level. We have assumed that before the pump pulse is applied, all the electrons are in the ground level, i.e. $N_0 = N$. This assumption is well justified at temperature of 4 K, where all the donors are fully ionised.

$$\frac{dN_0(t)}{dt} = -\frac{\sigma_0}{\hbar\omega} I(t)N_0(t) + \frac{\sigma_0}{\hbar\omega} I(t)N_i(t) + \frac{N_i(t)}{\tau_{i0}} + \frac{N_c(t)}{\tau_{c0}} \quad (1)$$

$$\frac{dN_i(t)}{dt} = \frac{\sigma_0}{\hbar\omega} I(t)N_0(t) - \frac{\sigma_0}{\hbar\omega} I(t)N_i(t) - \frac{\sigma_i}{\hbar\omega} I(t)N_i(t) + \frac{\sigma_i}{\hbar\omega} I(t)N_c(t) - \frac{N_i(t)}{\tau_{i0}} + \frac{N_c(t)}{\tau_{ci}} \quad (2)$$

$$N_0(t) + N_i(t) + N_c(t) = N \quad (3)$$

The electron lifetime between energy levels is given as τ_{xy}, where subscript index x and y refer to the energy levels they represent respectively. σ_0 and σ_i are the absorption cross-sections from E_0 to E_i and E_i to E_c respectively. ω is the photon circular frequency of the pump pulse. The pump pulse $I(t)$ with respect of time t can be best described using a sech function with a peak intensity of I_0 and full width at half maximum (FWHM) of τ_ω, $I(t) = I_0\, sech(t/0.38\tau_\omega)$. We have used a value of 0.7 ps for τ_ω in our model, which is reasonably close to the FELIX micropulse [11]. The last term in the right hand side of Equation 2, which counts the electron recombination rate from E_c to E_i, can be omitted. This omission is practical since electrons that relaxed to the excited subbands before further relaxed to the ground subband were almost indistinguishable from those electrons that relaxed directly from the continuum band to the ground subband. Hence, the actual occupation time of electrons in the continuum band may be a composite of τ_{ci} and τ_{c0}. In addition, the stimulated term from the continuum conduction band to the excited subbands (forth term in Equation 2) can be omitted too. In the pump-probe experiment, the free electrons in the continuum conduction band were captured in the barrier and optical transition back to

the excited subbands should be minimum due to the spatial separation between the electron states. Our simulation further shows that there is no significant difference in omitting this term.

$$S(t_d) = \int_{-\infty}^{+\infty} K \cdot I(t - t_d) \cdot \exp\left[-\sigma_0(N_0 - N_i) + \sigma_i(N_i - N_c) + \sigma_c(N_c)\right] dt_d \qquad (4)$$

Equation 4 models the transmission of the probe signal as a function of time delay between the pump and the probe signal where K is an arbitrary constant. The pump and probe pulses in our pump-probe experiment are of the same origin albeit different intensity. Hence, the probe pulse, represented as $I(t-t_d)$ after a time delay t_d with respect to t of the pump pulse, will have the same wavelength, pulse duration, and pulse shape as the pump pulse. The absorption cross section in the continuum conduction band is denoted as σ_c.

With the parameters listed in Table 1, we have fitted the experimental result for both samples one and two. As depicted in figure 6, the fitted result for both samples agrees well with the experimental data. Fitting of data from sample two gave a 2.5 ps intersubband lifetime and a 700 ps slow decay lifetime. It is noticeable that in all cases the strong, long lifetime negative signal is always preceded by a short lifetime, positive saturation signal. The model also reproduces all the features observed in figure 4 where reducing the pump intensity will reduce, and eventually elliminate the strong negative signal, as shown in figure 7. In some cases (e.g. figure 6.b and figure 6.d), there is evidence of a two-component decay (τ_2 and τ_3 in figure 4) to the absorption signal whose detailed origin is unknown. The two-time-constant decay is probably associated with the dynamics of the electrons in the disturbed barrier potential (figure 5).

5. CONCLUSIONS

Pump-probe lifetime measurements have been made on two GaAs/AlGaAs samples containing 50 and 80 stepped quantum wells. The results show that electrons in the samples have longer intersubband lifetimes than normal rectangular QWs. For high intensity pump pulses, multi-photon absorption can occur. It becomes significant when the multi-photon absorption energy coincides with the resonant energy of the ground subband to the barrier. The free electrons induced by multi-photon absorption result in very strong absorption of the pump light. This would lead to a serious additional loss mechanism in optically pumped far infrared lasers. It can be greatly reduced by ensuring that the stepped quantum well requires more than two photons to ionise it. Although weak residual absorption attributed to three photon absorption is detectable in such structures, it is not of practical importance.

ACKNOWLEDGEMENTS

The authors are sincerely grateful to the EPSRC for funding the research and to the EPSRC Central Facility for III-V Semiconductors at the University of Sheffield for providing the samples. The authors gratefully acknowledge the support of Stichting voor Fundamenteel Onderzoek der Materie (FOM) in providing the required beam time on FELIX and highly appreciate the skilful assistance of the FELIX staff, in particular Dr A.F.G. van der Meer.

Table 1: Parameters and corresponding values used in the rate equation model for fitting the pump-probe measurement data for both sample one and two.

Parameters	Symbols	Sample one values	Sample two values
Total population	N_0	$1 \times 10^{11}\ cm^{-2}$	$1 \times 10^{12}\ cm^{-2}$
Cross section in E_0 to E_i absorption	σ_0	$2.6 \times 10^{-15}\ cm^2$	$2.6 \times 10^{-15}\ cm^2$
Cross section in E_i to E_c absorption	σ_i	$0.8 \times 2.6 \times 10^{-15}\ cm^2$	$0.8 \times 2.6 \times 10^{-15}\ cm^2$
Cross section in E_c absorption	σ_c	$150 \times 2.6 \times 10^{-15}\ cm^2$	$150 \times 2.6 \times 10^{-15}\ cm^2$
Intersubband electron lifetime	τ_{i0}	1.8 ps	2.5 ps
Continuum band to ground subband lifetime	τ_{c0}	550 ps	700 ps
Pump wavelength	λ_ω	10.6 μm	9.35 μm
Pump pulse width	τ_ω	0.7 ps	0.7 ps

LIST OF FIGURES

and drift to the doping region. ΔE_{c0} indicates the energy gap between the ground subband and the bottom of the continuum conduction band.

Figure 6. The pump-probe intersubband lifetime measurement (circles) for sample one with the solid lines fitted using the rate equation model with intersubband lifetime of 1.8 ps (a) and the slow decay fitted with a lifetime of 550 ps (b). The corresponding intersubband lifetime for sample two is 2.5ps (c) with a 700 ps slow decay lifetime.

Figure 7. Simulated pump-probe signal with varying pump intensities using the rate equation model. The strong negative signal disappears when large attenuation is introduced to the pump pulse.

REFERENCES

[1] B. F. Levine, J. Appl. Phys., **74**, R1 (1993).

[2] Z. Xin and H. N. Rutt, Semicond. Sci. Technol., **12,** 1129 (1997).

[3] S. Borenstain and J. Katz, Appl. Phys. Lett., **55**, 654 (1989).

[4] O. Gauthier-Lafaye, F. H. Julien, S. Cabaret, J. –M Lourtioz, G. Strasser, E. Gornik, M. Helm and P. Bois, Appl. Phys. Lett., **74**, 1537 (1999).

[5] B. N. Murdin, G. M. H. Knippels, A. F. G. van der Meer, C. R. Pidgeon, C. J. G. M. Langerak, M. Helm, W. Heiss, K Unterrainer, E. Gornik, K. K. Geerinck, N. J. Hovenier and W. Th. Wenckebach, Semicond. Sci. Technol., **9**, 1554 (1994).

[6] A. Seilmeier, H. –J. Hubner, G. Abstreiter, G. Weimann and W. Schlapp, Phys. Rev. Lett., **59**, 1345 (1987).

[7] K. L. Schumacher, D. Collings, R. T. Phillips, D. A. Ritchie, G. Weber, J. N. Schulman and K. Ploog, Semicond. Sci. Technol., **11**, 1173 (1996).

[8] K. L. Vodopyanov, V. Chazapis and C. C. Phillips, Appl. Phys. Lett., **69**, 3405 (1996).

[9] O. Gauthier-Lafaye, S. Sauvage, P. Boucaud, F. H. Julien, R. Prazeres, F. Glotin, J. –M. Ortega, V. Thierry-Mieg, R. Planel, J. –P. Leburton and V. Berger, Appl. Phys. Lett. **70,** 3197 (1997).

[10] P. C. Findlay, C. R. Pidgeon, R. Kotitschke, A. Hollingworth, B. N. Murdin, C. J. G. M. Langerak, A. F. G. van der Meer, C. M. Ciesla, J. Oswald, A. Homer, G. Spingholz and G. Bauer, Phys. Rev. B, **58**, 12908 (1998).

[11] The Infrared User Facilities FELIX, FOM-Institute for Plasma Physics "Rijnhuizen", The Netherlands, http://www.rijnh.nl/n4/n3/f1234.htm (2001)

[12] I-H. Tan, G. L. Snider, L. D. Chang and E. L. Hu, J. Appl. Phys., **68**, 4071 (1990).

[13] J. Faist, F. Capasso, C. Sirtori, D. L. Sivco, A. L. Hutchinson, S. N G. Chu and A. Y. Cho, Appl. Phys. Lett. **63**, 1354 (1993).

[14] R. A. Kaindl, K. Reimann, M Woerner, T. Elsaesser, R. Hey and K. H. Ploog, Phys. Rev. B, **63**, 161308-1 (2001).

[15] S. Lutgen, R. A. Kaindl, M. Woerner, T. Elsaesser, A. Hase and H. Kunzel, Phys. Rev. B, **54**, R17343 (1996).

[16] E. Dupont, P. Corkum, H. C. Liu, P. H Wilson, M. Buchanan and Z. R. Wasilewski, Appl. Phys. Lett. **65**, 1560 (1994).

[17] G. B.Serapiglia, E. Paspalakis, C. Sirtori, K. L. Vodopyanov, and C. C. Phillips, Phys. Rev. Lett., **84**, 1019 (2000).

[18] J. B. Khurgin, Semiconductors and Semimetals, Vol **59**, Ed E. Garmire and A Kost, Academic Press, 1999, Chapter One.

[19] E. Rosencher and Ph. Bois, Phys. Rev. B, **44**, 11315 (1991).

Figure 1

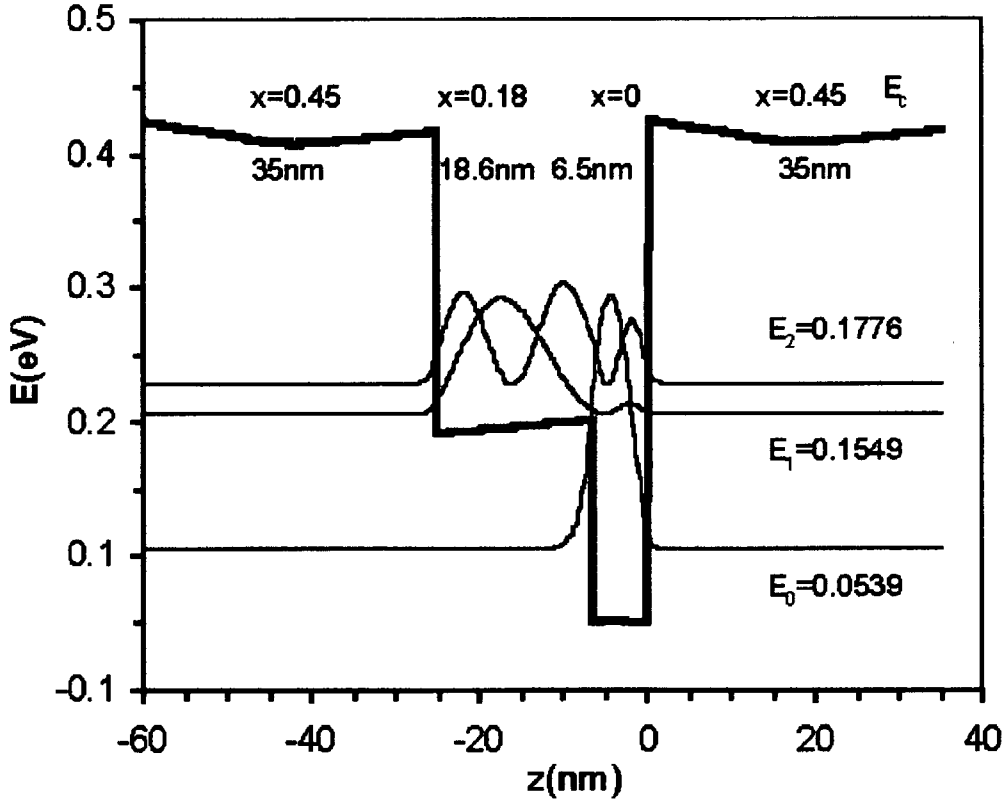

Figure 2

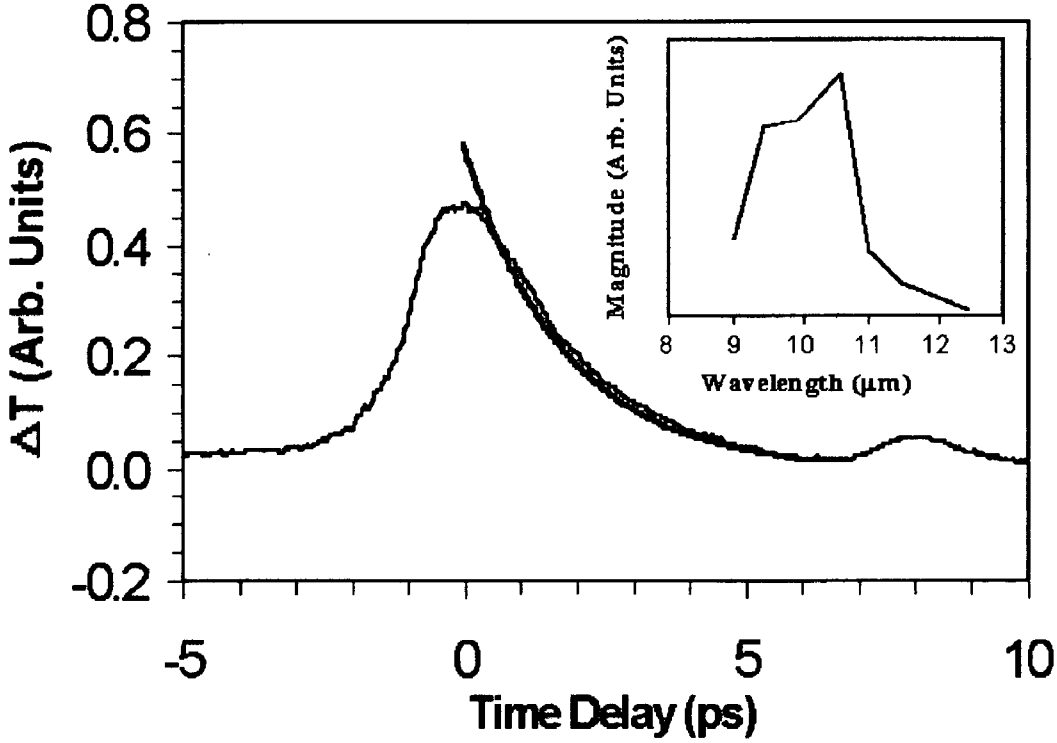

Tan et al, Intersubband lifetimes and free carrier effects in optically pumped far infrared quantum wells laser structures

Figure 3

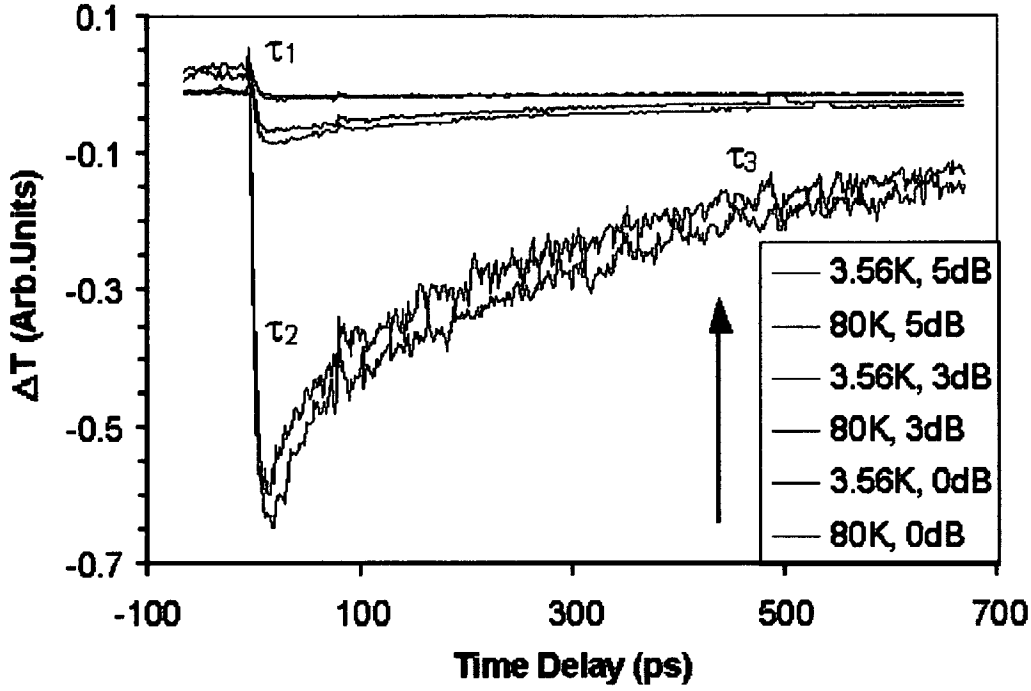

Figure 4

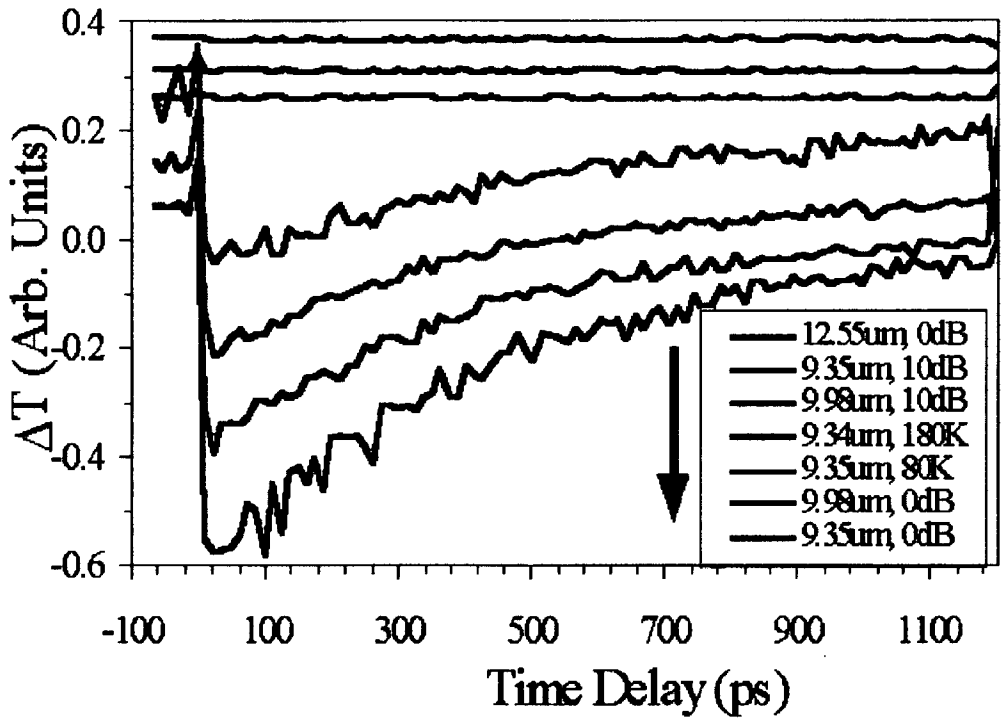

Figure 5

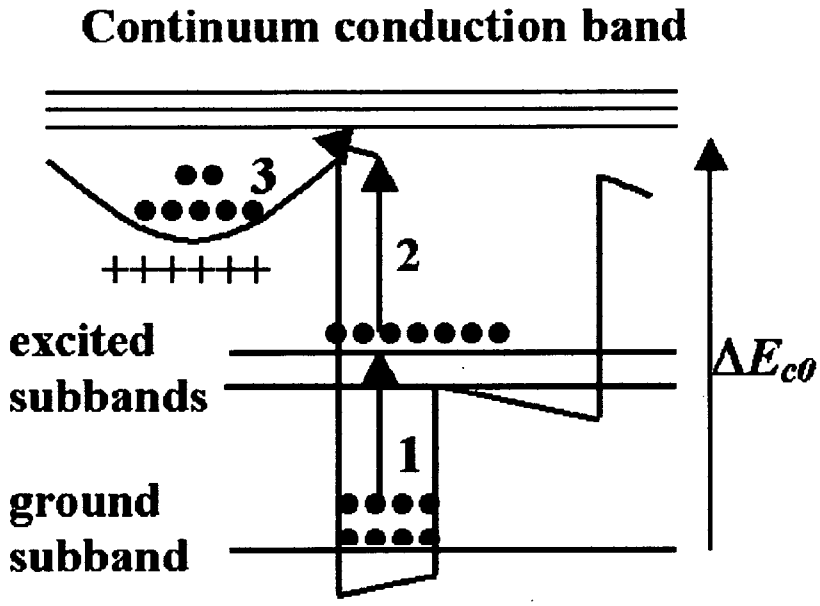

Figure 6

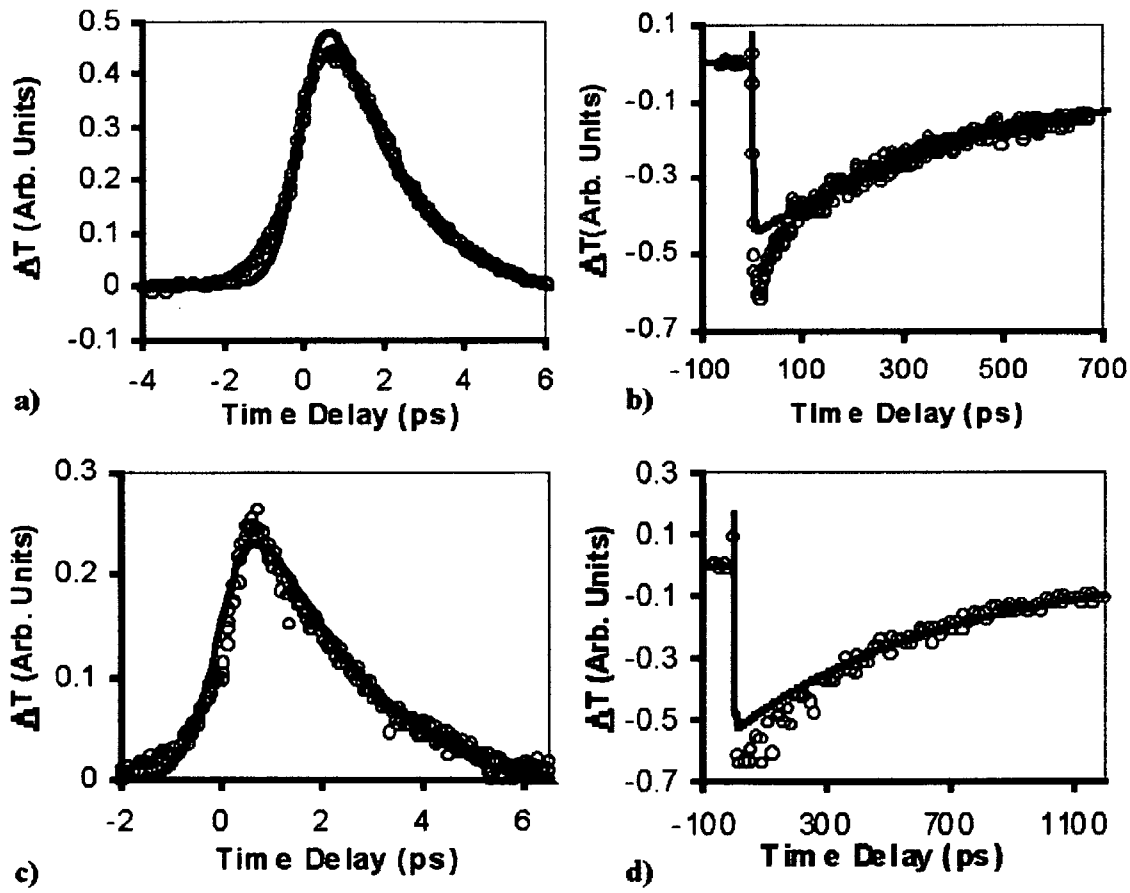

Tan et al, Intersubband lifetimes and free carrier effects in optically pumped far infrared quantum wells laser structures

Figure 7